

1

2 Title: An oxalate efflux transporter from the brown-rot fungus *Fomitopsis palustris*

3 Running title: Oxalate transporter from *Fomitopsis palustris*

4 Tomoki Watanabe<sup>1</sup>, Nobukazu Shitan<sup>1,3</sup>, Shiro Suzuki<sup>2</sup>, Toshiaki Umezawa<sup>1,2</sup>, Mikio  
5 Shimada<sup>1,4</sup>, Kazufumi Yazaki<sup>1</sup>, and Takefumi Hattori<sup>1\*</sup>

6 <sup>1</sup>*Research Institute for Sustainable Humanosphere, Kyoto University, Uji, Kyoto 611-0011,*  
7 *Japan;*

8 <sup>2</sup>*Institute of Sustainable Science, Kyoto University, Uji, Kyoto 611-0011, Japan;*

9 <sup>3</sup>*Present address: Laboratory of Natural Medicinal Chemistry, Kobe Pharmaceutical*  
10 *University, 4-19-1 Motoyamakita-machi, Higashinada-ku, Kobe 658-8558, Japan;*

11 <sup>4</sup>*Present address: Environmental and Biotechnological Frontier Engineering, Fukui*  
12 *University of Technology, Fukui 910-8505, Japan*

13 \*Address correspondence to: Takefumi Hattori, Research Institute for Sustainable  
14 Humanosphere, Kyoto University, Uji, Kyoto 611-0011, Phone: +81 774 38 3626. Fax: +81  
15 774 38 3682. E-mail address: [thattori@rish.kyoto-u.ac.jp](mailto:thattori@rish.kyoto-u.ac.jp)

16

17 Journal Section: Mycology

18

19 Abstract

20 An oxalate-fermenting brown-rot fungus, *Fomitopsis palustris*, secretes large amounts  
21 of oxalic acid during wood decay. Secretion of oxalic acid is indispensable for the  
22 degradation of wood cell walls, but almost nothing is known about the transport mechanism  
23 by which oxalic acid is secreted from *F. palustris* hyphal cells. We characterized the  
24 mechanism for oxalate transport using membrane vesicles of *F. palustris*. Oxalate transport  
25 in *F. palustris* was ATP dependent and was strongly inhibited by several inhibitors such as  
26 valinomycin and  $\text{NH}_4^+$ , suggesting the presence of a secondary oxalate transporter in this  
27 fungus. We then isolated a cDNA, *Fomitopsis palustris* Oxalic Acid Resistance (*FpOAR*),  
28 from *F. palustris* by functional screening of yeast transformants with cDNAs grown on  
29 oxalic acid-containing plates. FpOAR is predicted to be a membrane protein that possesses  
30 six transmembrane domains, but shows no similarity with known oxalate transporters. The  
31 yeast transformant possessing *FpOAR* (*FpOAR*-transformant) acquired resistance to oxalic  
32 acid and contained less oxalate than the control transformant. Biochemical analyses using  
33 membrane vesicles of the *FpOAR*-transformant showed that the oxalate transport property  
34 of FpOAR was consistent with that observed in membrane vesicles of *F. palustris*. The  
35 quantity of *FpOAR* transcripts was correlated with increasing oxalic acid accumulation in  
36 the culture medium and was induced when exogenous oxalate was added to the medium.  
37 These results strongly suggest that FpOAR plays an important role in wood decay by acting  
38 as a secondary transporter responsible for secretion of oxalate by *F. palustris*.

39

40 Oxalic acid is produced by a wide variety of members of five kingdoms (*Monera*, *Protista*,  
41 *Fungi*, *Plantae*, and *Animalia*) (32), and plays multiple roles as a proton and electron  
42 source and strong metal chelator in ecosystem processes (11). With regard to wood decay  
43 by brown-rot fungi, which cause severe damage to wooden structures, oxalic acid is  
44 secreted by the fungus in large amounts (8, 38). Several important roles of oxalic acid in the  
45 brown-rot decay process are proposed. Oxalic acid hydrolyzes side-chains of  
46 hemicelluloses, then depolymerizes the hemicellulose backbones and amorphous cellulose,  
47 thus increasing the porosity of the wood structure to the hyphal sheath, decay enzymes, or  
48 other low-molecular-weight decay agents (12). In cellulose degradation by the Fenton  
49 reaction, a low concentration of oxalate promotes degradation (41) by facilitating hydroxyl  
50 radical formation (45), but a higher concentration of the acid inhibits the degradation (41)  
51 and radical formation (45). Furthermore, oxalate forms Fe-oxalate complexes, which can  
52 then diffuse into the wood cell wall for the Fenton reaction by which oxalate protects the  
53 hyphae of brown-rot fungi from attack by the Fenton reagent (2, 16, 38). Therefore, from  
54 the viewpoint of preservation of wooden buildings and cultural treasures, elucidation of the  
55 biochemical mechanisms for oxalate biosynthesis and its secretion in brown-rot fungi is  
56 needed.

57 Recently, we clarified the mechanisms for oxalate biosynthesis in the brown-rot  
58 basidiomycete *Fomitopsis palustris*, which is used as a standard fungus for Japanese  
59 Industrial Standards decay resistance tests. *Fomitopsis palustris* secretes large amounts of  
60 oxalate (33–78 mM) into the culture fluid, which lowers the medium pH to ca. 2. The  
61 terminal enzymes for oxalate biosynthesis are cytosolic oxaloacetate acetylhydrolase

62 (OAAH, EC 3.7.1.1) (1) and peroxisomal cytochrome *c* dependent glyoxylate  
63 dehydrogenase (15, 43). Our biochemical analysis of oxalate fermentation by *F. palustris*  
64 led to the conclusion that the fungus acquires energy for growth by oxidizing glucose  
65 mainly to oxalate through the tricarboxylic acid (TCA) and glyoxylate (GLOX) cycles (28,  
66 29, 35).

67 Importantly, it is widely recognized that oxalate is toxic to organisms. Exogenously  
68 added oxalate inhibits sporulation and growth of the filamentous fungi *Fusarium*  
69 *oxysporum* (7) and *Pythium vexans* (46). Therefore, oxalate-producing brown-rot fungi  
70 must have a mechanism to prevent damage caused by intra- and extra-cellular oxalate.  
71 Several brown-rot fungi show not only oxalate-producing but also oxalate-degrading  
72 activity. Among these oxalate-producing and -degrading brown-rot fungi, *Postia placenta*  
73 produces oxalate decarboxylase to convert oxalate to formate and CO<sub>2</sub> (25), which prevents  
74 overaccumulation of oxalic acid and forms a non-toxic, buffered, low-pH environment that  
75 facilitates the brown-rot decay process (26). *Gloephyllum trabeum* degrades extracellularly  
76 added oxalate to give rise to CO<sub>2</sub> (10). Similarly, *Fomitopsis pinicola* and *Meruliporia*  
77 *incrassata* have been reported to decrease the amount of extracellular oxalate (36).

78 In contrast to these oxalate-producing and -degrading brown-rot fungi,  
79 oxalate-decomposing activity has not been reported for *F. palustris*. However, *F. palustris*  
80 grows vigorously in the presence of a high oxalate concentration (28, 29). The marked  
81 accumulation of oxalic acid in the culture fluid of *F. palustris* suggests that the fungus has  
82 an efficient system to transport oxalate out of the cells. Oxalate is continuously  
83 biosynthesized as a major end product of primary metabolism in the cytosol and

84 peroxisome of *F. palustris* (15, 28, 35). Thus, while transporting oxalate from the  
85 peroxisome to the cytosol and eventually out of the cells, essential metabolic processes  
86 should be protected from oxalate toxicity. In this context, the oxalate transporter in the  
87 cytosolic membrane is expected to reduce the intracellular concentration of oxalate, which  
88 probably contributes to the oxalate resistance system in *F. palustris*. However, almost  
89 nothing is known about the transport systems of *F. palustris*.

90 Oxalate transporters are known to play several important roles in metabolizing or  
91 excreting oxalate by other organisms. For example, *Oxalobacter formigenes*, a  
92 gram-negative anaerobe, possesses the oxalate:formate exchange protein OxIT, which is  
93 essential for *O. formigenes* to produce ATP (21). Humans and mice possess the SLC26  
94 multifunctional anion exchangers, of which SLC26A6 (humans) and Slc26a6 (mice) are  
95 proposed to exchange Cl<sup>-</sup> and SO<sub>4</sub><sup>2-</sup> for oxalate or formate in the intestinal villi, renal  
96 proximal tubule and cardiac myocytes (27). Furthermore, hepatopancreatic lysosomal  
97 membrane vesicles isolated from the lobster *Homarus americanus* exchange oxalate for Cl<sup>-</sup>  
98 in relation to Zn<sup>2+</sup> detoxification (40).

99 Recently, Mch5, a homolog of a putative oxalate:formate antiporter from *Aspergillus*  
100 *fumigatus*, was postulated to be a putative oxalate transporter in yeast *Saccharomyces*  
101 *cerevisiae*. However, the oxalate-transporting activity of Mch5 and the possible roles of the  
102 gene product have not been demonstrated (5). Accordingly, an oxalate-transporting protein  
103 has not previously been characterized experimentally from any fungus.

104 Here we describe a cDNA encoding the protein involved in oxalate transport in *F.*  
105 *palustris*. To isolate a cDNA encoding the oxalate transporter, we previously isolated

106 fungal cDNAs from yeast transformants with cDNA of *F. palustris* grown in the presence  
107 of a high oxalate concentration that is lethal to wild-type cells (49). Even if oxalate was  
108 incorporated into the cells, the transformants probably transported oxalate out of the cells or  
109 it was degraded by the gene products of the cDNA from *F. palustris*. Accordingly, these  
110 cDNAs were expected to encode transporters catalyzing oxalate transport out of the cells or  
111 oxalate-decomposing enzymes and other proteins possessing unidentified functions. By this  
112 strategy, we successfully isolated the cDNA *FpTRP26* conferring oxalic acid resistance for  
113 *F. palustris* (49). We have further characterized the remaining transformants showing oxalic  
114 acid resistance (49) and obtained the gene product, FpOAR (*Fomitopsis palustris* Oxalic  
115 Acid Resistance), which is a putative plasma membrane protein that showed distinct  
116 oxalate transport activity in yeast membrane vesicles. The oxalate transport property of  
117 FpOAR was similar to that of *F. palustris* membrane vesicles. These results strongly  
118 suggest that FpOAR is involved in oxalate secretion in *F. palustris* hyphal cells.

119

120

## MATERIALS AND METHODS

121

122 ***Fomitopsis palustris* culture conditions.** Two mycelial plugs (5 mm in diameter) of *F.*  
123 *palustris* (Berkely et Curtis) Murill TYP6137 were grown as a stationary culture in a 200  
124 ml Erlenmeyer flask containing 40 ml liquid medium as previously reported (49).

125 **Cloning of *F. palustris* cDNA conferring oxalic acid resistance.** Functional screening  
126 of a *Saccharomyces cerevisiae* AD12345678 (6) transformant with a *F. palustris* cDNA  
127 library with vector pDR196 (51) was carried out to screen the transformants to grow with

128 12 mM oxalic acid (49). Because the cDNA fragment recovered from oxalic acid-resistant  
129 yeast showing a strong phenotype lacked the 5' region, the 5' end of the cDNA was  
130 determined with the Gene Racer™ kit (Invitrogen) according to the manufacturer's  
131 instructions. The 5' end of the cDNA was cloned with the gene-specific antisense PCR  
132 primer 5'-CCACGACCACCGCCGCAAGCATGAAGA-3'. The amplified cDNA fragments  
133 were subcloned into the TA cloning vector with the pCR2 TOPO TA cloning kit  
134 (Invitrogen). A clone containing an insert of the expected size was sequenced. The open  
135 reading frame (ORF) of the cDNA was cloned with the PCR primers  
136 5'-ACTAGTATGACCGACCTGCATCGAAG-3' (sense) and  
137 5'-GGATCCTCAGAGAAGATCTTCTTGCCG-3' (antisense), which were gene-specific  
138 primers containing *Spe* I and the *Bam*HI restriction site, respectively. The coding region  
139 thus obtained was named *FpOAR* (*Fomitopsis palustris* Oxalic Acid Resistance).

140 **Characterization of oxalic acid-resistance activity of FpOAR.** The plasmid  
141 containing *FpOAR* was reintroduced into the *S. cerevisiae* AD12345678 strain to  
142 characterize its oxalic acid resistance according to our method reported previously (49).  
143 Oxalic acid resistance was determined by growth of the yeast transformant. Similarly, the  
144 transformants were cultivated separately on SD (-Ura) plates containing different HCl  
145 concentrations (pH 1.5, 1.6, and 2.2).

146 **Quantification of oxalic acid.** Oxalic acid in the *F. palustris* culture medium was  
147 quantified with a commercial kit after the pH of the medium was adjusted for the assay  
148 (Roche, Germany) (48), while GC-MS analysis (14) was conducted for that in yeast cells.  
149 Yeast (OD<sub>600</sub> 0.1) was cultured at 30°C in 50 ml SD (-Ura) liquid medium containing 2

150 mM oxalic acid until OD<sub>600</sub> 1.0–2.0. The cells were harvested by centrifugation at 1000×g  
151 for 10 min and washed twice with cold distilled water. The dry weight of cells was  
152 determined after freeze-drying for 5 h. To the dried cells, 250 µl 1N HCl and 600 µl  
153 ethylacetate were added and cells were homogenized with glass beads (Toshinriko, No. 04)  
154 for 4 min. The oxalic acid extracted with ethylacetate was quantified as previously  
155 described (14).

156 GC-MS (EI) was performed on a Shimadzu GC-MS QP-5050A. The column conditions  
157 were as follows: CBP1-M25-025, 25 m × 0.22 mm (i.d.) (Shimadzu), column temperature  
158 80–240°C (8°C/min), carrier gas He, and carrier gas flow rate 0.8 ml/min.

159 **Quantitative real-time PCR analysis of gene transcription.** Total RNA was isolated  
160 from *F. palustris* mycelia with the RNeasy Plant Mini Kit (Qiagen). First-strand cDNA  
161 synthesis was performed with Superscript II reverse transcriptase (Invitrogen) using 0.2 µg  
162 RNA. Real-time quantitative PCR was performed with a 7300 Real Time System (Applied  
163 Biosystems) and amplicons were detected with SYBR Green (Applied Biosystems).  
164 Quantifications of the amplicons were based on standard curves prepared for each target  
165 cDNA. The gene-specific primers 5'-CCTCGAACAAGCGAATTCTCTTT-3' and  
166 5'-AGTGTCCCGCCGAGGAA-3' were used to generate an 85 bp amplicon for *FpOAR*  
167 transcripts. The amount of transcripts was normalized by comparison with those of a 75 bp  
168 amplicon derived from either total RNA or 28S rRNA (GenBank accession no. AY515333)  
169 with the primers 5'-TGACACGGACTACCAGTGCTTT-3' (sense) and  
170 5'-CACCCATTTTGAGCTGCATTC-3' (antisense).



171 *FpOAR* transcripts were quantified in mycelia from cultures to which either oxalate (50  
172 mM final concentration) or H<sub>2</sub>O was added on day 3. The cultures were incubated for 12 h  
173 prior to RNA extraction.

174 **Preparation of *F. palustris* membrane vesicles.** The membrane vesicles were prepared  
175 from *F. palustris* hyphal cells as described previously (33). Cells were collected and  
176 homogenized in ice-cold homogenizing buffer (0.1 M Tris-HCl, pH 8.0, 10% [v/v] glycerol,  
177 5 mM EDTA; 2 ml/g fresh weight of mycelia) using a Phoenix blender (USA). Prior to use,  
178 KCl, DTT, and PMSF were added to the autoclaved buffer at the final concentrations 150  
179 mM, 3.3 mM and 1 mM, respectively, and the mixture was stirred for 1 min. Unbroken  
180 cells and debris were removed by centrifugation twice at 8,000×g for 10 min. The  
181 supernatants were pooled and centrifuged at 100,000×g for 60 min. The microsome fraction  
182 was resuspended with autoclaved resuspension buffer (10 mM Tris-HCl, pH 7.6, 10% [v/v]  
183 glycerol, 1 mM EDTA). Isolated membrane vesicles were stored at –80°C in resuspension  
184 buffer containing 1 mM DTT and 1 mM PMSF until use.

185 Yeast membrane vesicles for *in vitro* transport studies were isolated as described  
186 previously (17, 44) with the following modifications. The *S. cerevisiae* AD12345678 strain  
187 was grown overnight in SD (–Ura) liquid medium to OD<sub>600</sub> 1–2. Cells were washed twice  
188 with water and resuspended to OD<sub>600</sub> 1–2 in spheroplast buffer (1.1 M sorbitol, 20 mM  
189 Tris-HCl [pH 7.6], 1 mM DTT containing 57 units/ml Zymolyase 20T). After cell wall  
190 digestion was completed, spheroplasts were collected by centrifugation at 1200×g for 10  
191 min. Cell lysis was performed gently on ice in 25 ml breaking buffer (1.1 M glycerol, 50  
192 mM Tris-ascorbate [pH 7.4], 5 mM EDTA, 1 mM DTT, 1.5% polyvinylpyrrolidone, 2

193 mg/ml BSA, 1 mM PMSF, 10 µg/ml leupeptin, 2 µg/ml aprotinin, and 2 µg/ml pepstatin)  
194 with a Dounce homogenizer and 40 strokes with a tight-fitting glass piston. Unbroken cells  
195 and debris were removed by centrifugation twice at 3,000×g for 10 min. The supernatants  
196 were pooled and centrifuged at 100,000×g for 60 min. Microsomal membrane proteins  
197 were quantified by Bradford's method (3). The pellet was suspended to a protein  
198 concentration of about 5 mg/ml in vesicle buffer (1.1 M glycerol, 50 mM Tris-MES [pH  
199 7.4], 1 mM EDTA, 1 mM DTT, 2 mg/ml BSA, 1 mM PMSF, 1 µg/ml leupeptin, 2 µg/ml  
200 aprotinin, and 2 µg/ml pepstatin). Small aliquots were immediately used for transport  
201 assays or stored at -80°C until use. Membrane vesicles prepared with this method are a  
202 mixture of inside-out and right-side-out orientation, whereas only inside-out vesicles can  
203 hydrolyze ATP owing to the outside orientation of the ATPase catalytic sites that drive  
204 membrane transport and because ATP cannot permeate the membrane. Therefore, in this  
205 experiment the observation of oxalate uptake into the inside-out vesicle indicates oxalate  
206 efflux activity of the hyphal cell membrane.

207 ***In vitro* oxalate transport assay.** Vesicles (100 µg protein) were mixed with transport  
208 buffer (0.4 M glycerol, 100 mM KCl, 20 mM Tris-MES [pH 7.4], 1 mM DTT) and  
209 incubated with 0.2 mM [<sup>14</sup>C]oxalic acid at 25 °C for 10 min in the absence or presence of 5  
210 mM MgATP with a final volume of 125 µl, unless stated otherwise. In the assay using *F.*  
211 *palustris* vesicles, the vesicles (500 µg protein) were suspended in a final volume of 500 µl.  
212 Uptake of [<sup>14</sup>C]oxalic acid (185 MBq/mmol) into membrane vesicles was measured by two  
213 methods. For *F. palustris* membrane vesicles, 130 µL reaction mixture was loaded on a  
214 Sephadex (G-50 fine) spin column and centrifuged at 2,000 rpm for 2 min. The

215 radioactivity of 100  $\mu$ L filtrate was determined with a liquid scintillation counter. The yeast  
216 vesicles were absorbed onto nitrocellulose filters (3 cm in diameter, 0.45  $\mu$ m pore size; GE  
217 Healthcare) by filtration with an aspirator. The vesicles on the membrane were washed  
218 three times with 1 ml transport buffer by filtration with an aspirator, dried on filter paper  
219 and subjected to liquid scintillation counting. Counts were corrected for background and  
220 quenching. Quantification and calculations were performed using a Liquid Scintillation  
221 Analyzer Tri-Carb 2800TR (Perkin Elmer, USA).

222 **Effects of inhibitors on oxalate transport.** Using *F. palustris* vesicles, the following  
223 inhibitors were added separately to assay solutions: 1 mM vanadate, 2  $\mu$ M valinomycin, 1  
224 mM  $\text{NH}_4\text{Cl}$ , 150  $\mu$ M glibenclamide, or 5  $\mu$ M cyclosporin A. Oxalate transport was  
225 recorded as described above.

226 To assess the inhibition using yeast vesicles from the *FpOAR*-transformant, we used 5  
227  $\mu$ M verapamil, and 5  $\mu$ M gramicidin D in addition to the reagents used for the *F. palustris*  
228 vesicle assay. Oxalate transport was recorded as described above.

229 **Statistical analysis.** Analyses were carried out using ANOVA followed by the Dunnett  
230 test with a level of significance of  $p = 0.05$ .

231

232

## RESULTS

233

234 **Biochemical analysis of oxalate transport using *F. palustris* membrane vesicles.** To  
235 characterize oxalate transport of *F. palustris* we prepared membrane vesicles from hyphae  
236 of the fungus and investigated whether MgATP is required for the transport activity. In the

237 presence of MgATP, [<sup>14</sup>C]oxalate uptake into the vesicles was 4.27 times that in the control  
238 lacking MgATP (Fig. 1). This result indicated that MgATP is needed for oxalate transport  
239 activity in *F. palustris*.

240 We then investigated the effects of a variety of inhibitors on oxalate transport. Vanadate,  
241 which is an inhibitor of P-type ATPases and ATP-binding cassette (ABC) transporters,  
242 reduced oxalate uptake into the membrane vesicle by 68.0%. The addition of valinomycin  
243 or NH<sub>4</sub>Cl, which abolish the  $\Delta\Psi$  and  $\Delta\text{pH}$  across the membrane, respectively, inhibited  
244 oxalate uptake by 86.3% and 90.1%, respectively. In contrast, glybenclamide and  
245 cyclosporin A, which are typical inhibitors of ABC transporters, did not influence oxalate  
246 transport. These results indicate that ABC transporters are not primarily responsible for  
247 oxalate transport. Collectively, the results strongly suggest that a secondary oxalate  
248 transporter functions in *F. palustris*, in which  $\Delta\Psi$  and  $\Delta\text{pH}$  are involved.

249 **Cloning of a cDNA conferring oxalic acid resistance on the yeast transformant.**

250 Previously, we isolated the cDNA FpTRP26 from one of eight *S. cerevisiae* transformants  
251 (49). From the remaining transformants, we isolated one cDNA (1170 bp), named *FpOAR*  
252 (GenBank accession no. AB372882), which was found to encode a deduced 42,873 Da  
253 protein. A BLASTp (<http://www.ncbi.nlm.nih.gov/BLAST/>) search revealed that the  
254 deduced FpOAR showed 86%, 82%, 73%, 66% and 43% identities with predicted  
255 membrane proteins of *Postia placenta* (24) and *Phanerochaete chrysosporium* (23), a major  
256 intrinsic protein of *Laccaria bicolor* (22), a hypothetical protein CC1G\_06363 of  
257 *Coprinopsis cinerea* Okayama 7#130 (4), and a transmembrane protein of *Cryptococcus*  
258 *neoformans* var. *neoformans* JEC21 (19), respectively (Fig. 2). These are all basidiomycete

259 fungi and, in particular, *P. placenta* and *P. chrysosporium* are brown- and white-rot fungi,  
260 respectively. However, no biochemical functions have been elucidated for these proteins to  
261 date. A close similarity between FpOAR and oxalate-degrading enzymes, such as oxalate  
262 decarboxylase (EC 4.1.1.2) and oxalate oxidase (EC 1.2.3.4), was not observed. However,  
263 the SOSUI program (<http://bp.nuap.nagoya-u.ac.jp/sosui/>) predicted that FpOAR possesses  
264 six transmembrane domains (Supplemental Fig. S1).

265 **Oxalic acid resistance in yeast transformants with the cDNA FpOAR.** On plates  
266 containing 8.5–10 mM oxalic acid, the yeast transformant possessing the cDNA *FpOAR*  
267 (*FpOAR*-transformant) showed clear cell growth, whereas no growth was observed in the  
268 control transformant with an empty vector (Figs. 3A, B). At an oxalic acid concentration  
269 below 8.5 mM, the growth of the control and *FpOAR*-transformant did not differ  
270 significantly (data not shown). In medium with the same pH containing malonate but not  
271 oxalate, no difference between the control and *FpOAR*-transformant was observed, showing  
272 that oxalate is more toxic than malonate (Fig. 3C). To eliminate the possibility that the  
273 *FpOAR*-transformant was resistant to low pH (2.2–1.5), we investigated the growth of the  
274 *FpOAR*-transformant on a low-pH plate (Fig. 3D), but no difference in growth between the  
275 control and *FpOAR*-transformant was observed at pH 2.2–1.5 and pH 5. We then compared  
276 the oxalic acid contents of the *FpOAR*-transformant and the empty vector control grown in  
277 the presence of 2 mM oxalic acid. No difference in cell growth was observed between the  
278 two cultures at this concentration, but the cellular content of oxalate in the  
279 *FpOAR*-transformant strongly decreased to 25% compared with that of the control (Fig. 4).

280 **Oxalate transport in vesicles of the *FpOAR*-transformant.** In the presence of

281 MgATP, membrane vesicles of the *FpOAR*-transformant significantly accumulated  
282 [<sup>14</sup>C]oxalate, which was 1.4 times greater than that of the control lacking MgATP. When  
283 the assay was conducted at 4 °C or with vesicles denatured at 95 °C, oxalate transport did  
284 not differ from that of the empty vector control (Fig. 5).

285 Vanadate and gramicidin D, which are inhibitors of P-type ATPases and a  
286 monovalent-selective ionophore that dissipates both the pH gradient and membrane  
287 potential, inhibited oxalate transport by 28.5% and 55.8%, respectively (Fig. 6).  
288 Valinomycin and NH<sub>4</sub>Cl, which abolish  $\Delta\Psi$  and  $\Delta\text{pH}$  across the membrane, respectively,  
289 inhibited oxalate transport by 34.6% and 34.9%, respectively. In contrast, the inhibitors of  
290 ABC transporters, glybenclamide and verapamil, slightly inhibited and did not  
291 significantly inhibit, respectively, oxalate transport in *FpOAR*-transformant vesicles. These  
292 results are in agreement with the oxalate-transporting activity exhibited by membrane  
293 vesicles of *F. palustris* (Fig. 1), and suggest that *FpOAR* is directly involved in oxalate  
294 secretion.

295 **Quantitative real-time PCR analysis of *FpOAR* transcripts in *F. palustris*.** The  
296 quantity of *FpOAR* transcripts increased concomitantly with accumulation of oxalate in the  
297 culture medium (Figs. 7A, B and C). High levels were maintained even in the stationary  
298 phase during days 9–13, while oxalic acid accumulation increased (day 13, 34 mM). The  
299 amount of *FpOAR* transcripts increased three-fold compared with that of the control when  
300 50 mM oxalic acid was added to the medium (Fig. 8).

301

302

## DISCUSSION

303 **FpOAR functions as a secondary oxalate transporter conferring oxalic acid**  
304 **resistance in *F. palustris*.** In this study, we characterized oxalate transport using membrane  
305 vesicles of *F. palustris*. We isolated a cDNA, *FpOAR*, encoding a novel membrane oxalate  
306 transporter protein specifically conserved among basidiomycete fungi.

307 The isolated cDNA *FpOAR* conferred resistance to oxalic acid on the  
308 *FpOAR*-transformant (Figs. 3A, B, C and D). The oxalate transport activity in the  
309 membrane vesicles of the yeast (Fig. 5) indicated that FpOAR was responsible for oxalate  
310 transport. The effects of inhibitors on oxalate transport in membrane vesicles of the  
311 *FpOAR*-transformant (Fig. 6) suggest that FpOAR transports oxalate by a secondary  
312 transport system, in which  $\Delta\text{pH}$  and  $\Delta\Psi$  are the driving force. The effects of the inhibitors  
313 on yeast vesicles (Fig. 6) were similar to those on vesicles from *F. palustris* (Fig. 1).  
314 Furthermore, expression of *FpOAR* and oxalic acid accumulation in the medium were  
315 positively correlated (Fig. 7A, B and C). Expression of *FpOAR* was induced by addition of  
316 oxalic acid to the culture (Fig. 8). Collectively, these results strongly suggest the  
317 involvement of FpOAR as a secondary oxalate transporter to confer oxalic acid resistance  
318 in *F. palustris*.

319 **FpOAR is a plasma membrane-localized novel secondary oxalate transporter.**  
320 FpOAR is proposed to be a novel oxalate secondary transporter based on three lines of  
321 evidence: 1) MgATP was needed for oxalate transport activity; 2) FpOAR does not possess  
322 an ATP-hydrolyzing domain (Walker motifs and ABC signature) as in ABC transporters,  
323 which function as primary transporters (47); and 3) there is no similarity between FpOAR  
324 and known oxalate transporters, e.g. SLC26 family proteins (27), the oxalate:formate

325 antiport protein, OxIT (21), and the putative yeast monocarboxylate transporter, Mch5 (5).

326 FpOAR is suggested to be a plasma membrane oxalate efflux transporter based on the  
327 lower oxalate content in the *FpOAR*-transformant compared with the control (Fig. 4). The  
328 probable cytosolic membrane localization of FpOAR is in agreement with the presence of  
329 six putative transmembrane domains in FpOAR (Supplemental Fig. S1). Furthermore, the  
330 PSORT program (<http://psort.hgc.jp/>) predicted that FpOAR is localized to the plasma  
331 membrane. The fungal plasma membrane H<sup>+</sup>-ATPase generates a proton gradient through  
332 the cytosolic membrane (37), which is likely to drive oxalate transport through FpOAR.

333 **FpOAR probably plays a crucial role to maintain carbon metabolism by *F.***  
334 ***palustris*.** During vegetative growth, *F. palustris* produces oxalate from a glucose carbon  
335 source with an 80% theoretical yield based on the amount of carbon in glucose (28). Two  
336 intrinsic features of *F. palustris* metabolism facilitate such a high yield of oxalate. First, the  
337 precursors of oxalate, glyoxylate and oxaloacetate, are constantly supplied through the  
338 GLOX cycle in the peroxisome, in which isocitrate lyase (FPICL1, EC 4.1.3.1) and malate  
339 synthase (EC 2.3.3.9) play indispensable roles as key enzymes (28, 29, 35). The FPICL1  
340 and malate synthase of *F. palustris* show high activity even in glucose-grown mycelia (28,  
341 29), which is in sharp contrast to the general GLOX cycle in other microorganisms, in  
342 which the functioning of the GLOX cycle is repressed by a glucose carbon source (35).  
343 Second, it is proposed that the GLOX cycle of *F. palustris* supplies succinate constitutively  
344 to the TCA cycle lacking 2-oxoglutarate dehydrogenase activity (28, 29, 35), by which  
345 oxaloacetate can be supplied for cytosolic oxalate production through the TCA cycle as  
346 well as the GLOX cycle (28, 29, 35).



347 *Fomitopsis palustris* continuously secretes oxalate as the fungus grows. This oxalate  
348 secretion is mainly due to continuous production of oxalate in primary carbon metabolism.  
349 Furthermore, the acid secretion could be due to the absence of oxalate degradation activity  
350 in *F. palustris*, in contrast to oxalate-decomposing white-rot fungi (9, 39, 48, 50) and  
351 several brown-rot fungi such as *P. placenta* (25) and *G. trabeum* (10). Moreover, we have  
352 suggested that *F. palustris* transports oxalate out of the cells to prevent possible inhibition  
353 of intracellular metabolic reactions. For example, oxalate might inhibit the activities of  
354 FPICL1 and malate synthase in peroxisomes of *F. palustris* (15, 35), because oxalate  
355 competitively inhibits the activities of the two enzymes *in vitro* (30, 31). In addition,  
356 oxalate produced from oxaloacetate by cytosolic OAAH in *F. palustris* (1, 35) possibly  
357 shows product inhibition for OAAH activity, because oxalate is a competitive inhibitor ( $K_i$   
358 = 19  $\mu$ M) for OAAH from *Botrytis cinerea* (13). Therefore, the oxalate production coupled  
359 with energy metabolism and the efficient oxalate transport out of the cells are essential to  
360 maintain carbon metabolism in *F. palustris*. Aided by the oxalate export system, including  
361 FpOAR, and the oxalic acid resistance system, including FpTRP26 (49), carbon  
362 metabolism through the TCA and GLOX cycles are probably prevented from inhibition by  
363 oxalate *in vivo*. FpTRP26 was predicted to be a soluble protein and might help with oxalate  
364 export from the hyphal cells (49). The yeast transformant with FpTRP26 showed similar  
365 resistance to oxalic acid with regard to the acid concentration and pH (49). Further research  
366 is needed to elucidate how FpTRP26 and FpOAR cooperatively work in the oxalate  
367 resistance system. Whether the FpOAR homologous protein functions in oxalate-producing  
368 and -degrading brown-rot fungi requires investigation. Furthermore, in the same fungi, a

369 possible role of oxalate degradation in relation to energy metabolism should be evaluated to  
370 clarify the possible role of oxalate metabolism in brown-rot fungi. In this context, a  
371 possible ATP-generation by oxalate degradation is hypothesized for *P. placenta* (20) based  
372 on gene expression (24) as proposed for white-rot oxalate-degrading fungus *C.*  
373 *subvermispora* in which oxalate degradation by oxalate decarboxylase with formate  
374 dehydrogenase could produce NADH to be utilized for ATP synthesis (48).

375 **FpOAR homologous protein is a potential target for development of new wood**  
376 **preservatives.** The FpOAR homologous protein may be distributed widely in wood-rotting  
377 fungi, because the homologs showing significant identities with FpOAR were found in  
378 genomes of the brown- and white-rot fungi *P. placenta* and *P. chrysosporium*, respectively  
379 (Fig. 2). Oxalate production and secretion is commonly observed in wood-rotting fungi,  
380 although brown-rot fungi accumulate greater amounts of oxalate in the culture fluid than do  
381 white-rot fungi (8, 38). Therefore, the FpOAR homologous protein may generally function  
382 as an oxalate transporter in wood-rotting fungi. From the viewpoint of wood preservation,  
383 if the function of FpOAR is inhibited by wood preservatives, oxalate is expected to be  
384 accumulated intracellularly in brown-rot fungi and growth would be seriously damaged. By  
385 a similar inhibitory mechanism, oxalate excretion by white-rot fungi would decrease, which  
386 may repress lignin degradation, because a certain amount of excreted oxalate is important  
387 to stabilize  $Mn^{3+}$  oxidation for lignin degradation by manganese peroxidase (18).  
388 Accordingly, the FpOAR homologous protein would be a possible target protein to develop  
389 a new wood preservative to inactivate oxalate transport for extermination of wood-rotting  
390 fungi.

391 In summary, we have isolated a cDNA, *FpOAR*, encoding a novel oxalate transporter  
392 from *F. palustris*. The deduced FpOAR protein is suggested to play an important role in  
393 wood decay by acting as a secondary transporter responsible for secretion of oxalate from *F.*  
394 *palustris* hyphal cells. Two strategies for prevention of oxalate toxicity have been found for  
395 brown-rot fungi: 1) oxalate efflux through FpOAR; and 2) in addition to oxalate efflux,  
396 oxalate degradation in oxalate-producing and -degrading brown-rot fungi. Further  
397 characterization of oxalate transport by FpOAR is needed to elucidate the underlying  
398 mechanisms. Oxalate transport from the peroxisome to the cytosol remains to be  
399 investigated.

400

## REFERENCES

401

- 402 1. **Akamatsu, Y., A. Ohta, M. Takahashi, and M. Shimada.** 1991. Enzymatic  
403 formation of oxalate from oxaloacetate with cell-free-extracts of the brown-rot  
404 fungus *Tyromyces palustris* in relation to the biodegradation of cellulose.  
405 *Mokuzai Gakkaishi* **37**:575-577.
- 406 2. **Arantes, V., Y. Qian, A. M. F. Milagres, J. Jellison, and B. Goodell.** 2009.  
407 Effect of pH and oxalic acid on the reduction of Fe<sup>3+</sup> by a biomimetic chelator  
408 and on Fe<sup>3+</sup> desorption/adsorption onto wood: Implications for brown-rot decay.  
409 *International Biodeterioration & Biodegradation* **63**:478-483.
- 410 3. **Bradford, M. M.** 1976. Rapid and sensitive method for quantitation of  
411 microgram quantities of protein utilizing principle of protein-dye binding. *Anal.*  
412 *Biochem.* **72**:248-254.
- 413 4. **Broad Institute of MIT and Harvard.** 2003. *Coprinus cinereus* sequencing  
414 project (<http://www.broad.mit.edu>).
- 415 5. **Cheng, V., H. U. Stotz, K. Hippchen, and A. T. Bakalinsky.** 2007.  
416 Genome-wide screen for oxalate-sensitive mutants of *Saccharomyces cerevisiae*.  
417 *Appl. Environ. Microbiol.* **73**: 5919-5927.
- 418 6. **Decottignies, A., A. M. Grant, J. W. Nichols, H. de Wet, D. B. Mcintosh, and**  
419 **A. Goffeau.** 1998. ATPase and multidrug transport activities of the overexpressed  
420 yeast ABC protein Yor1p. *J. Biol. Chem.* **273**:12612-12622.
- 421 7. **Duchesne, L.C., B. E. Ellis, and R. L. Peterson.** 1989. Disease suppression by  
422 the ectomycorrhizal fungus *Paxillus involutus* –contribution of oxalic acid-. *Can.*  
423 *J. Bot.* **67**: 2726-2730.
- 424 8. **Dutton, M. V., and C. S. Evans.** 1996. Oxalate production by fungi: Its role in

- 425 pathogenicity and ecology in the soil environment. *Can. J. Microbiol.*  
426 **42**:881-895.
- 427 9. **Escutia, M. R., I. Bowater, A. Edwards, A. R. Bottrill, M. R. Burrnull, R.**  
428 **Polanco, R. Vicuña, and S. Bornemann.** 2005. Cloning and Sequencing of two  
429 *Ceriporiopsis subvermispora* bicupin oxalate oxidase allelic isoforms:  
430 Implications for the reaction specificity of oxalate oxidases and decarboxylases.  
431 *Appl. Environ. Microbiol.* **71**:3608-3616.
- 432 10. **Espejo, E., and E. Agosin.** 1991. Production and degradation of oxalic acid by  
433 brown-rot fungi. *Appl. Environ. Microbiol.* **57**: 1980-1986.
- 434 11. **Gadd, G. M.** 2007. Geomycology: biogeochemical transformations of rocks,  
435 minerals, metals and radionuclides by fungi, bioweathering and bioremediation.  
436 *Mycol. Res.* **111**:3-49.
- 437 12. **Green III, F., M. J. Larsen, J. E. Winandy, and T. L. Highley.** 1991. Role of  
438 oxalic acid in incipient brown-rot decay. *Mater. Org.* **26**:191-213.
- 439 13. **Han, Y., H. J. Joosten, W. Niu, Z. Zhao, P. S. Mariano, M. T. McCalman, J.**  
440 **A. L. van Kan, P. J. Schaap, and D. Dunaway-mariano.** 2007. Oxaloacetate  
441 hydrolase, the C-C bond lyase of oxalate secreting fungi. *J. Biol. Chem.*  
442 **282**:9581-9590.
- 443 14. **Hattori, T., N. Akitsu, G. S. Seo, A. Ohta, and M. Shimada.** 2000. A possible  
444 growth promoting effect of the organic acids produced in an axenic symbiotic  
445 culture of *Pinus densiflora* and *Lactarius hatsudake* on both of symbionts. *Ann.*  
446 *Report. Interdiscipl. Res. Inst. Environ. Sci.* **19**:59-65.
- 447 15. **Hattori, T., K. Okawa, M. Fujimura, M. Mizoguchi, T. Watanabe, T.**  
448 **Tokimatsu, H. Inui, K. Baba, S. Suzuki, T. Umezawa, and M. Shimada.** 2007

- 449 Subcellular localization of the oxalic acid-producing enzyme, cytochrome  
450 *c*-dependent glyoxylate dehydrogenase in grown-rot fungus *Fomitopsis palustris*.  
451 Cellulose Chemistry and Technol. **41**:545-553.
- 452 16. **Hyde, S.M., and P.M. Wood.** 1997. A mechanism for production of hydroxyl  
453 radicals by the brown-rot fungus *Coniophora puteana*: Fe(III) reduction by  
454 cellobiose dehydrogenase and Fe(II) oxidation at a distance from the hyphae.  
455 Microbiology **143**: 259-266.
- 456 17. **Klein, M., Y. M. Mammun, T. Eggmann, C. Schüller, H. Wolfger, E.**  
457 **Martinoia, and K. Kuchler.** 2002. The ATP-binding cassette (ABC)  
458 transporter Bpt1p mediates vacuolar sequestration of glutathione conjugates in  
459 yeast. FEBS Letters **520**:63-67.
- 460 18. **Kuan, I. C., and M. Tien.** 1993. Stimulation of Mn-peroxidase activity - A  
461 possible role for oxalate in lignin biodegradation. Proc. Natl. Acad. Sci. USA  
462 **90**:1242-1246.
- 463 19. **Loftus, B.J., E. Fung, P. Roncaglia, D. Rowley, P. Amedeo, D. Bruno, J.**  
464 **Vamathevan, M. Miranda, I. J. Anderson, J. A. Fraser, J. E. Allen, I. E.**  
465 **Bosdet, M. R. Brent, R. Chiu, T. L. Doering, M. J. Donlin, C. A. D'Souza, D.**  
466 **S. Fox, V. Grinberg, J. Fu, M. Fukushima, B. J. Haas, J. C. Cuang, G.**  
467 **Janbon, S. J. M. Jones, H. L. Koo, M. I. Krzywinski, J. K. Kwon-Chung, K.**  
468 **B. Lengeler, R. Maiti, M.A. Marra, R. E. Marra, C. A. Mathewson, T. G.**  
469 **Mitchell, M. Pertea, F. R. Riggs, S. L. Salzberg, J. E. Schein, A.**  
470 **Shgvartsbeyn, H. Shin, M. Shumway, C. A. Specht, B. B. Suh, A. Tenney, T.**  
471 **R. Utterback, B. L. Wickes, J. R. Wortman, N. H. Wye, J. W. Kronstad, J. K.**  
472 **Lodge, J. Heitman, R. W. Davis, C. M. Fraser, R. W. Hyman.** 2005. The

- 473 genome of the basidiomycetous yeast and human pathogen *Cryptococcus*  
474 *neoformans*. Science **307**: 1321-1324.
- 475 20. **Mäkelä, M.R., K. Hildén, T. K. Lundell.** 2010. Oxalate decarboxylase:  
476 biotechnological update and prevalence of the enzyme in filamentous fungi. Appl.  
477 Microbiol. Biotechnol. **87**: 801-814.
- 478 21. **Malony, P.C.** 1994. Bacterial transporters. Current Opinion in Cell Biology  
479 **6**:571-582.
- 480 22. **Martin, F., A. Aerts, D. Ahréen, A. Brun, E. G. J. Danchin, F. Duchaussoy,**  
481 **J. Gibon, A. Kohler, E. Lindquist, V. Pereda, A. Salamov, H. J. Shapiro, J.**  
482 **Wuyts, D. Blaudez, M. Buée, P. Brokstein, B. Canbäck, D. Cohen, P. E.**  
483 **Courty, P. M. Coutinho, C. Delaruelle, J. C. Detter, A. Deveau, S. DiFazio, S.**  
484 **Duplessis, L. Fraissinet-Tachet, E. Lucic, P. Frey-Klett, C. Fourrey, I.**  
485 **Feussner, G. Gay, J. Grimwood, P. J. Hoegger, P. Jain, S. Kilaru, J. Labbé,**  
486 **Y. C. Lin, V. Legué, F. L. Tacon, R. Marmeisse, D. Melayah, B. Montanini,**  
487 **M. Muratet, U. Nehls, H. Niculita-Hirzel, M. P. Oudot-Le Secq, M. Peter, H.**  
488 **Quesneville, B. Rajashekar, M. Reich, N. Rouhier, J. Schmutz, T. Yin, M.**  
489 **Chalot, B. Henrissat, U. Kües, S. Lucas, V. de Peer, G. K. Podila, A. Polle, P.**  
490 **J. Pukkila, P. M. Richardson, P. Rouzé, I. R. Sanders, J. E. Stajich, A.**  
491 **Tunlid, G. Tuskan, I. V. Grigoriev.** 2008. The genome of *Laccaria bicolor*  
492 provides insights into mycorrhizal symbiosis. Nature **452**: 88-92.
- 493 23. **Martinez, D., L. F. Larrondo, N. Putnam, M. D. Gelpke, K. Huang, J.**  
494 **Chapman, K. G. Helfenbein, P. Ramaiya, J. C. Detter, F. Larimer, P. M.**  
495 **Coutinho, B. Henrissat, R. Berka, D. Cullen, D. Rokhsar.** 2004. Genome

- 496 sequence of the lignocelluloses degrading fungus *Phanerochaete chrysosporium*  
497 strain RP78. Nature Biotechnology **22**: 695-700.
- 498 24. **Martinez, D., J. Challacombe, I. Morgenstern, D. Hibbett, M. Schmoll, C. P.**  
499 **Kubicek, P. Ferreira, F. J. Ruiz-Duenas, A. T. Martinez, P. Kersten, K. E.**  
500 **Hammel, A. V. Wymelenberg, J. Gaskell, E. Lindquist, G. Sabat, S. S.**  
501 **BonDurant, L. F. Larrondo, P. Canessa, R. Vicuna, J. Yadav, H.**  
502 **Doddapaneni, V. Subramanian, A. G. Pisabarro, J. L. Laví, J. A. Oguiza, E.**  
503 **Master, B. Henrissat, P. M. Coutinho, P. Harris, J. K. Magnuson, S. E. Baker,**  
504 **K. Bruno, W. Kenealy, P. J. Hoegger, U. Kűes, P. Ramaiya, S. Lucas, A.**  
505 **Salamov, H. Shapiro, H. Tu, L. C. Chee, M. Misra, G. Xie, S. Teter, D. Yaver,**  
506 **T. James, M. Mokrejs, M. Pospisek, I. V. Grigoriev, T. Brettin, D. Rokhsar, R.**  
507 **Berka, D. Cullen.** 2009. Genome, transcriptome, and secretome analysis of  
508 wood decay fungus *Postia placenta* supports unique mechanisms of  
509 lignocelluloses conversion. Proc. Natl. Acad. Sci. USA **106**:1954-1959.
- 510 25. **Micales, J. A.** 1995. Oxalate decarboxylase in the brown-rot wood decay fungus  
511 *Postia placenta*. Mater. Org. **29**: 177-186.
- 512 26. **Micales, J. A.** 1997. Localization and induction of oxalate decarboxylase in the  
513 brown-rot wood decay fungus *Postia placenta*. International Biodeterioration &  
514 Biodegradation **39**: 125-132.
- 515 27. **Mount, D. B., and M. F. Romero.** 2004 The SLC26 gene family of  
516 multifunctional anion exchangers. Pflűgers Archive-Eur. J. Physiol. **447**:710-721.
- 517 28. **Munir, E., J. J. Yoon, T. Tokimatsu, T. Hattori, and M. Shimada.** 2001 A  
518 physiological role for oxalic acid biosynthesis in the wood-rotting basidiomycete  
519 *Fomitopsis palustris*. Proc. Natl. Acad. Sci. USA **98**:11126-11130.



- 520 29. **Munir, E., J. J. Yoon, T. Tokimatsu, T. Hattori, and M. Shimada.** 2001. New  
521 role for glyoxylate cycle enzymes in wood-rotting basidiomycetes in relation to  
522 biosynthesis of oxalic acid. *J. Wood Sci.* **47**:368-373.
- 523 30. **Munir, E., T. Hattori, and M. Shimada.** 2002. Purification and characterization  
524 of isocitrate lyase from the wood-destroying basidiomycete *Fomitopsis palustris*  
525 grown on glucose. *Arch. Biochem. Biophys.* **399**:225-231.
- 526 31. **Munir, E., T. Hattori, and M. Shimada.** 2002. Purification and characterization  
527 of malate synthase from the glucose-grown wood-rotting basidiomycete  
528 *Fomitopsis palustris*. *Biosci. Biotechnol. Biochem.* **66**:576-581.
- 529 32. **Nakata, P. A.** 2003. Advances in our understanding of calcium oxalate crystal  
530 formation and function in plants. *Plant Sci.* **164**:901-909.
- 531 33. **Otani, M., N. Shitan, K. Sakai, E. M. Martinoia, F. Sato, and K. Yazaki.**  
532 2005. Characterization of vacuolar transport of the endogenous alkaloid  
533 berberine in *Coptis japonica*. *Plant Physiol.* **138**:1939-1946.
- 534 34. **Page, R. D. M.** 1996. Tree View: An application to display phylogenetic trees on  
535 personal computers. *Comput. Appl. Biosci.* **12**:357-358.
- 536 35. **Sakai, S., T. Nishide, E. Munir, K. Baba, H. Inui, Y. Nakano, T. Hattori,**  
537 **and M. Shimada.** 2006. Subcellular localization of glyoxylate cycle key  
538 enzymes involved in oxalate biosynthesis of wood-destroying basidiomycete  
539 *Fomitopsis palustris* grown on glucose. *Microbiology* **152**:1857-1866.
- 540 36. **Schilling, J. S., and J. Jellison.** 2005. Oxalate regulation by two brown rot fungi  
541 decaying oxalate-amended and non-amended wood. *Holzforschung* **59**: 681-688.
- 542 37. **Serrano, R.** 1988. Structure and function of proton translocation ATPase in  
543 plasma membranes of plants and fungi. *Biochim. Biophys. Acta* **947**:1-28.

- 544 38. **Shimada, M., Y. Akamatsu, T. Tokimatsu, K. Mii, and T. Hattori.** 1997.  
545 Possible biochemical roles of oxalic acid as a low molecular weight compound  
546 involved in brown-rot and white-rot wood decays. *J. Biotechnol.* **53**:103-113.
- 547 39. **Shimazono, H.** 1955. Oxalic acid decarboxylase, a new enzyme from the  
548 mycelium of wood destroying fungi. *J. Biochem.* **42**:321-340.
- 549 40. **Sterling, K. M., P. K. Mandal, B. A. Roggenbeck, S. E. Ahearn, G. A.**  
550 **Gerencser, and G. A. Ahearn.** 2007. Heavy metal detoxification in crustacean  
551 epithelial lysosomes: role of anions in the compartmentalization process. *The*  
552 *Journal of Experimental Biology* **210**:3484-3493.
- 553 41. **Tanaka, N., Y. Akamatsu, T. Hattori, and M. Shimada.** 1994. Effect of oxalic  
554 acid on the oxidative break down of cellulose by the Fenton reaction. *Wood Res.*  
555 **81**:8-10.
- 556 42. **Thomson, J. D., T. J. Gibson, F. Plewhiak, F. Jeanmougin, and D. G.**  
557 **Higgins.** 1997. The CLUSTAL\_X windows interface: flexible strategies for  
558 multiple sequence alignment aided by quality analysis tools. *Nucleic Acid Res.*  
559 **25**:4876-4882.
- 560 43. **Tokimatsu, T., Y. Nagai, T. Hattori, and M. Shimada.** 1998. Purification and  
561 characteristics of a novel cytochrome *c* dependent glyoxylate dehydrogenase  
562 from a wood-destroying fungus *Tyromyces palustris*. *FEBS Letters*  
563 **437**:117-121.
- 564 44. **Tommasini, R., R. Evers, E. E. Vogt, C. Mornet, G. J. R. Zaman, A. H.**  
565 **Schinkel, P. Borst, and E. Martinoia.** 1996. The human multidrug  
566 resistance-associated protein functionally complements the yeast cadmium  
567 resistance factor 1. *Proc. Natl. Acad. Sci. USA* **93**: 6743-6748.

- 568 45. **Varela, E. and M. Tien.** 2003. Effect of pH and oxalate on  
569 hydroquinone-derived hydroxyl radical formation during brown rot wood  
570 degradation. *Appl. Environ. Microbiol.* **69**: 6025-6031.
- 571 46. **Yamaji, K., H. Ishimoto, N. Usui, and S. Mori.** 2005. Organic acids and  
572 water-soluble phenolics produced by *Paxillus* sp 60/92 together show antifungal  
573 activity against *Pythium vexans* under acidic culture conditions. *Mycorrhiza*  
574 **15**:17-23.
- 575 47. **Walker, J.E., M. Saraste, M. J. Runswick, and N. J. Gay.** 1982. Distantly  
576 related sequences in the alpha-subunits and beta-subunits of ATP synthase,  
577 myosin, kinases and other ATP-requiring enzymes and a common nucleotide  
578 binding fold. *EMBO J.* **1**:945-951.
- 579 48. **Watanabe, T., S. Tengku, T. Hattori, and M. Shimada.** 2005. Purification and  
580 characterization of NAD-dependent formate dehydrogenase from the white-rot  
581 fungus *Ceriporiopsis subvermispora* and a possible role of the enzyme in oxalate  
582 metabolism. *Enzyme Microb. Tech.* **37**:68-75.
- 583 49. **Watanabe, T., N. Shitan, T. Umezawa, K. Yazaki, M. Shimada, and T. Hattori.**  
584 2007. Involvement of FpTRP26, a thioredoxin-related protein, in oxalic  
585 acid-resistance of the brown-rot fungus *Fomitopsis palustris*. *FEBS Letters*  
586 **581**:1788-1792.
- 587 50. **Watanabe, T., T. Fujiwara, T. Umezawa, M. Shimada, and T. Hattori.** 2008.  
588 Cloning of a cDNA encoding a NAD-dependent formate dehydrogenase involved  
589 in oxalic acid metabolism from the white-rot fungus *Ceriporiopsis*  
590 *subvermispora* and its gene expression analysis. *FEMS Microbiol. Lett.*  
591 **279**:64-70.

592 51. **Wipf, D., M. Benjdia, E. Rikirsch, S. Zimmermann, M. Tegeder, and W. B.**  
593 **Frommer.** 2003. An expression cDNA library for suppression cloning in yeast  
594 mutants, complementation of a yeast his4 mutant, and EST analysis from the  
595 symbiotic basidiomycete *Hebeloma cylindrosporum*. *Genome* **46**:177-181.

596

597

#### ACKNOWLEDGMENTS

598

599 We thank Dr. A. Goffeau (Université Catholique de Louvain, Louvain-la-Neuve,  
600 Belgium) for kindly providing the *S. cerevisiae* strain AD12345678, and Dr. W.B.  
601 Frommer (Carnegie Institution, Stanford, CA, USA) for the gift of pDR196. This  
602 research was partly supported by a Grant-in-Aid for Scientific Research from the Japan  
603 Society for the Promotion of Science (No. 19580172), by a grant-in-aid from the  
604 Hokuto Foundation for Bioscience, and by a grant-in-aid from Development and  
605 Assessment of Sustainable Humanosphere (*DASH*)/Forest Biomass Analytical System  
606 (*FBAS*), *Kyoto University (20DF19 and 21DF19)*.

607

608 *The abbreviations used are: ABC, ATP-binding cassette; FpOAR, Fomitopsis palustris*  
609 *Oxalic Acid Resistance; GLOX, glyoxylate; TCA, tricarboxylic acid*

610

611

## Figure legends

612

613 FIG. 1. Oxalate transport and the effect of inhibitors using membrane vesicles from *F.*

614 *palustris*. Mean value  $\pm$  standard deviation.

615 \*  $p < 0.05$  ( $n = 3$ ).

616

617 FIG. 2. Neighbor-joining tree for FpOAR and its homologs. The tree was generated

618 using ClustalX (42) and visualized with TREEVIEW (34).

619 AAAY01000042, a transmembrane protein of *Cryptococcus neoformans* var.

620 *neoformans* JEC21 (GenBank accession no. AAAY01000042); gwh2.7.329.1, predicted

621 membrane proteins of *Phanerochaete chrysosporium* (JGI Protein ID 29288;

622 gwh2.7.329.1); Plus.C\_740045, predicted membrane proteins of *Postia placenta* (JGI

623 Protein ID 111900; estExt\_Genewise1Plus.C\_740045); FpOAR (*Fomitopsis palustris*

624 Oxalic Acid Resistance) (GenBank accession no. AB372882); Lbscf0011g04660, a

625 major intrinsic protein of *Laccaria bicolor* (JGI Protein ID 297309;

626 eu2.Lbscf0011g04660); AACs01000187, a hypothetical protein CC1G\_06363 of

627 *Coprinopsis cinerea* okayama 7#130 (GenBank accession no. AACs01000187).

628 Numbers at forks are bootstrap values derived from 1000 replicates. The scale bar


629 represents 0.05 substitutions per amino acid position.

630

631 FIG. 3. Growth of yeast transformants containing an empty vector (control) and *FpOAR*

632 on SD (-Ura) plates containing (A) no additives (standard), (B) oxalic acid, (C) malonic

633 acid and (D) HCl. Concentration of each additive and pH are shown above each image.

634 The number of yeast cells inoculated on the plate are indicated by  at the top of

635 each figure (A-D).

636

637 FIG. 4. Amount of oxalic acid in yeast transformants containing an empty vector  
638 (control) and *FpOAR*. Mean value  $\pm$  standard deviation. \*\*  $p < 0.01$  ( $n = 4$ ).

639

640 FIG. 5. Oxalate export in yeast transformants containing *FpOAR* (FpOAR-transformant)  
641 and an empty vector (control). \*\* $p < 0.01$  ( $n = 4$ ). The complete system,  
642 FpOAR-transformant + MgATP, showed significantly greater oxalate transport with \*\*  
643 than any other system. Denatured: the assay using the vesicles denatured at 95°C; 4°C:  
644 the assay conducted at 4°C. Mean value  $\pm$  standard deviation.

645

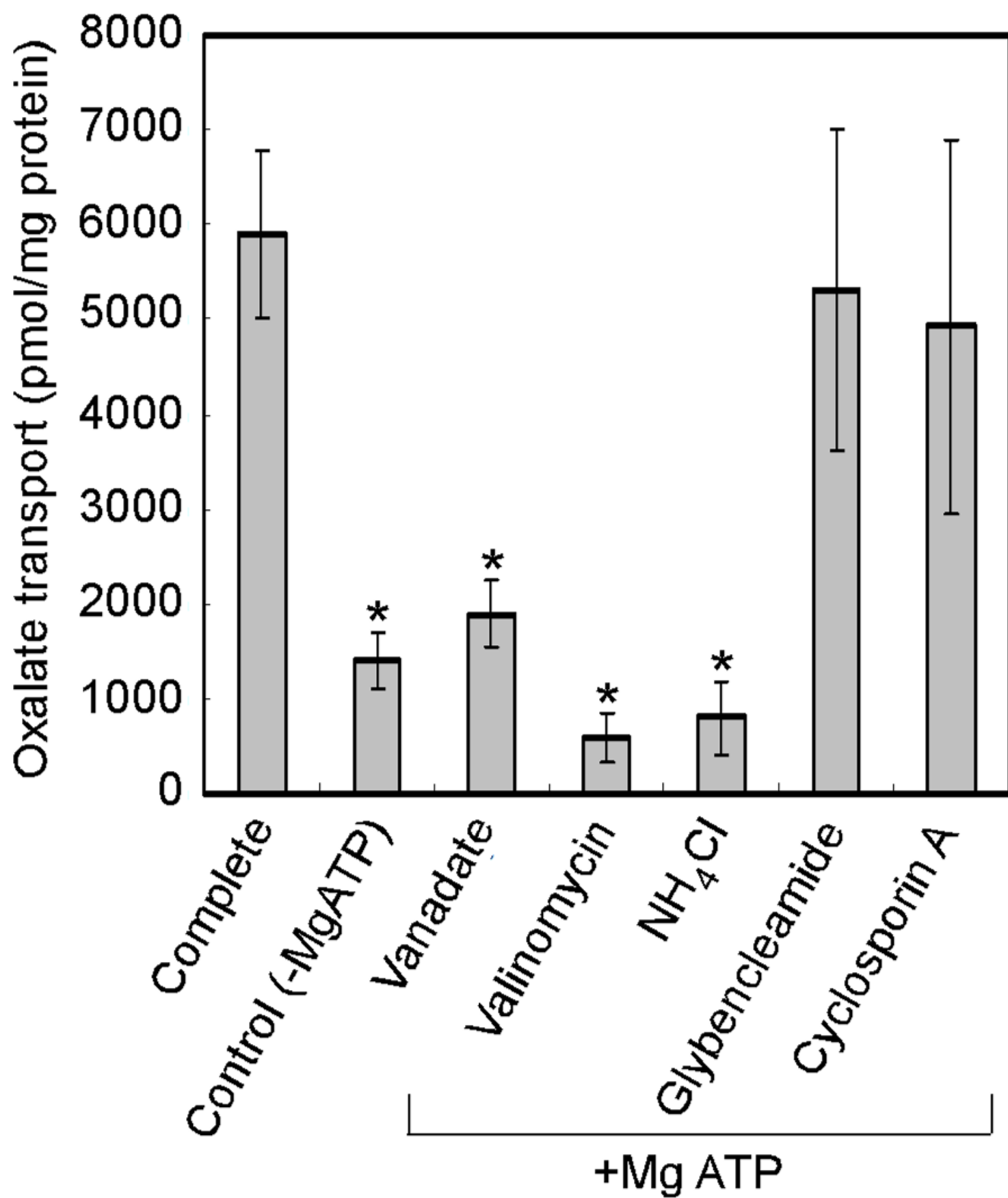
646 FIG. 6. Oxalate transport and effect of inhibitors using vesicles prepared from the  
647 *FpOAR*-transformant. The reaction was carried out for 20 min. Mean value  $\pm$  standard  
648 deviation. \*  $p < 0.05$  ( $n = 3$ ).

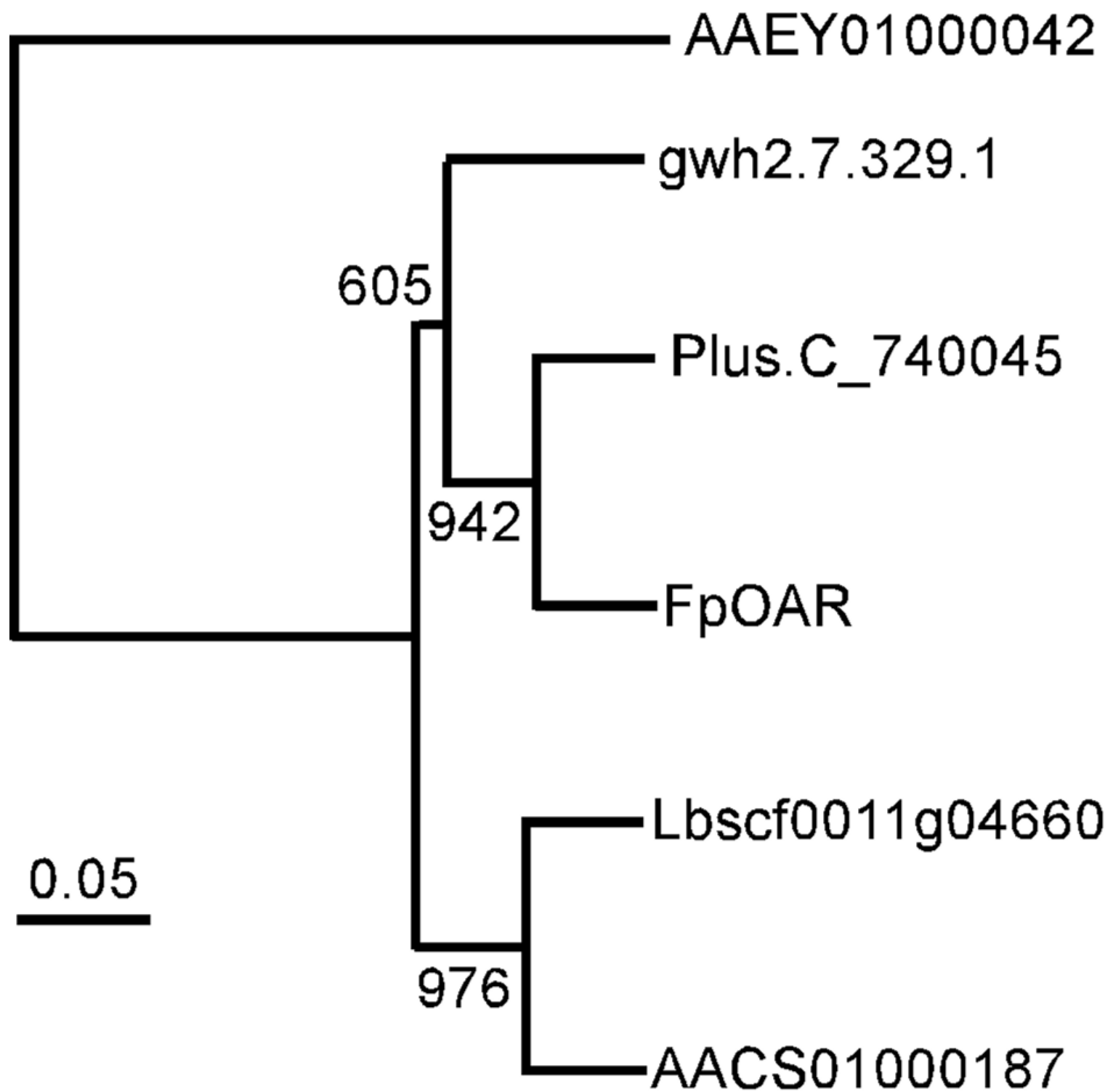
649

650 FIG. 7. Changes in (A) dry weight of mycelia, (B) oxalic acid accumulated and pH in  
651 the medium during culture of *F. palustris*. In (C) the copy number is shown based on 0.2  
652  $\mu$ g total RNA, where the copy number is defined as the number of molecules of mRNA  
653 coding FpOAR. The mean values and standard deviations were determined based on  
654 triplicate samples. Mean value  $\pm$  standard deviation.

655

656 FIG. 8. Effect of exogenous addition of oxalic acid to the *F. palustris* culture on *FpOAR*  
657 transcription. Mean value  $\pm$  standard deviation. \*\*  $p < 0.01$  ( $n = 4$ ).







(A) Standard

Cell density 

pH5.0

Control

*FpOAR*



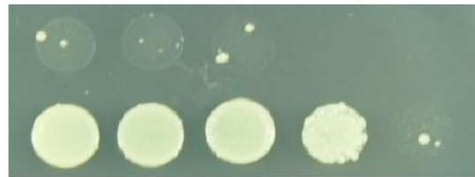
(B) Oxalic acid

Cell density 

8.5 mM (pH 2.5)

Control

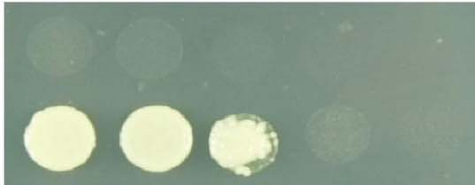
*FpOAR*



9.5 mM (pH 2.5)

Control

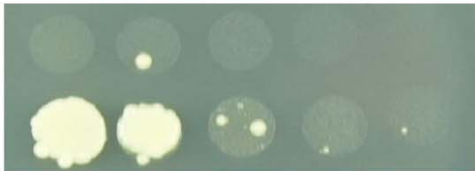
*FpOAR*



10 mM (pH 2.2)

Control

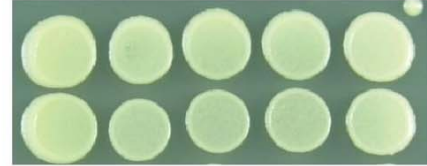
*FpOAR*



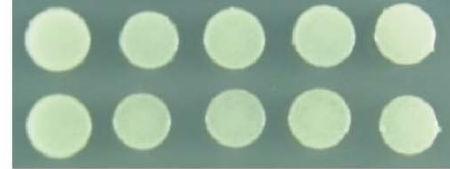
(C) Malonic acid



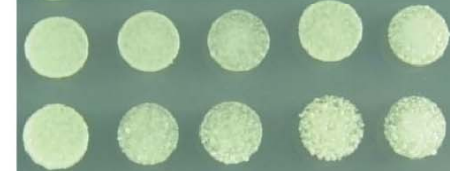
8.5 mM (pH 2.5)



9.5 mM (pH 2.5)



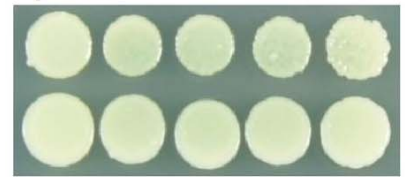
10 mM (pH 2.2)



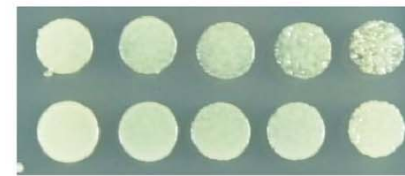
(D) Acidic pH



pH2.2

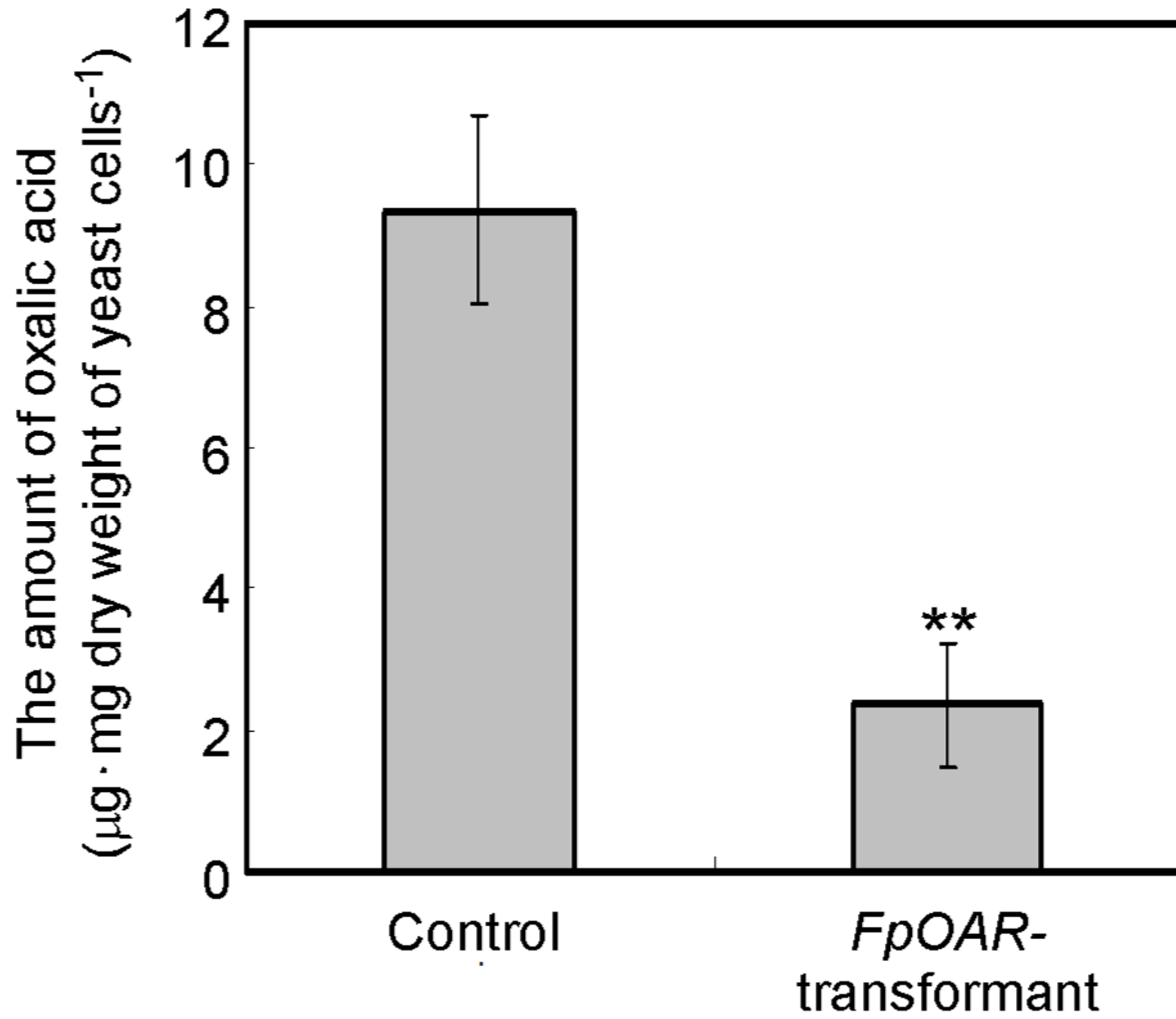


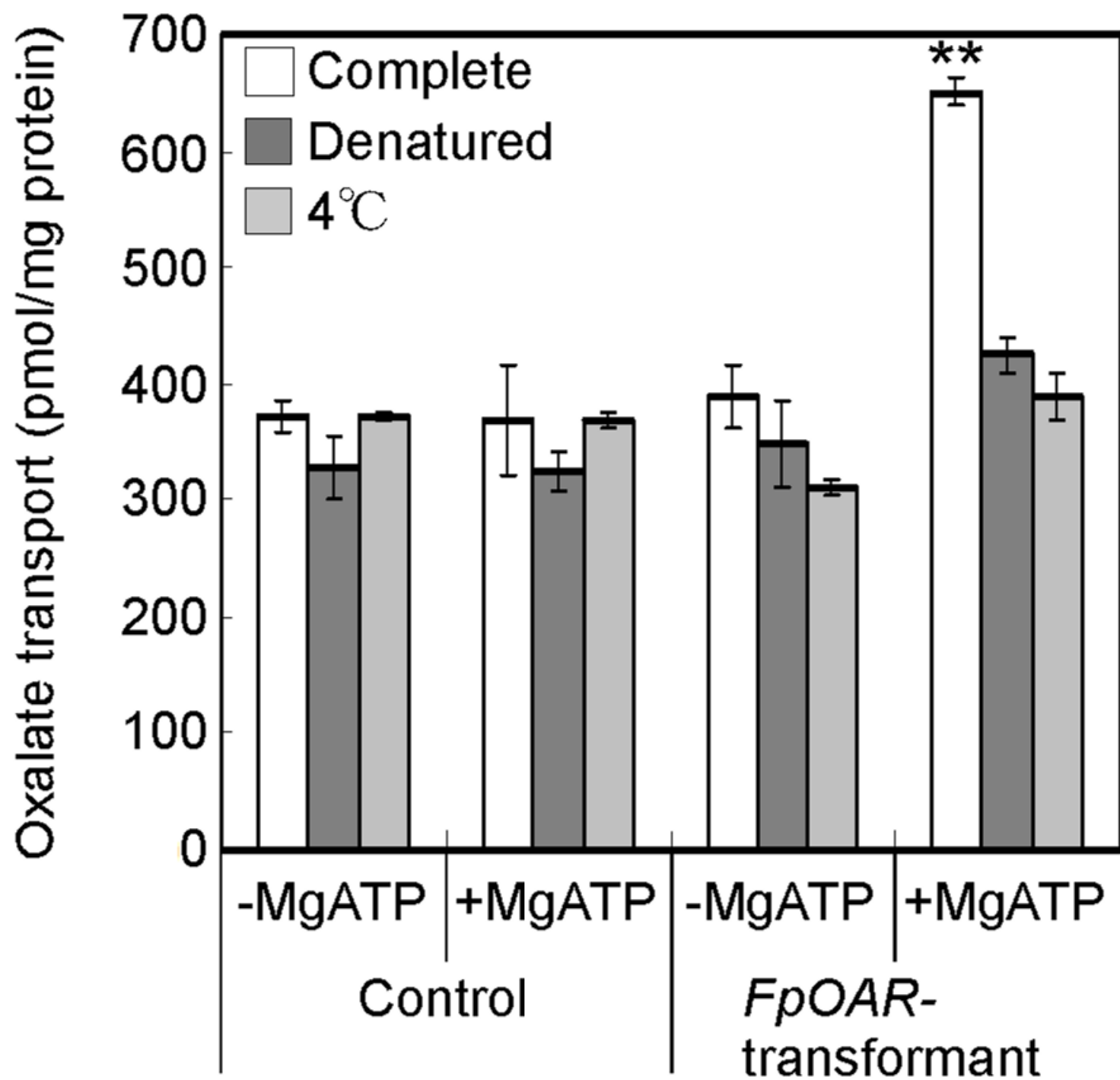
pH1.6

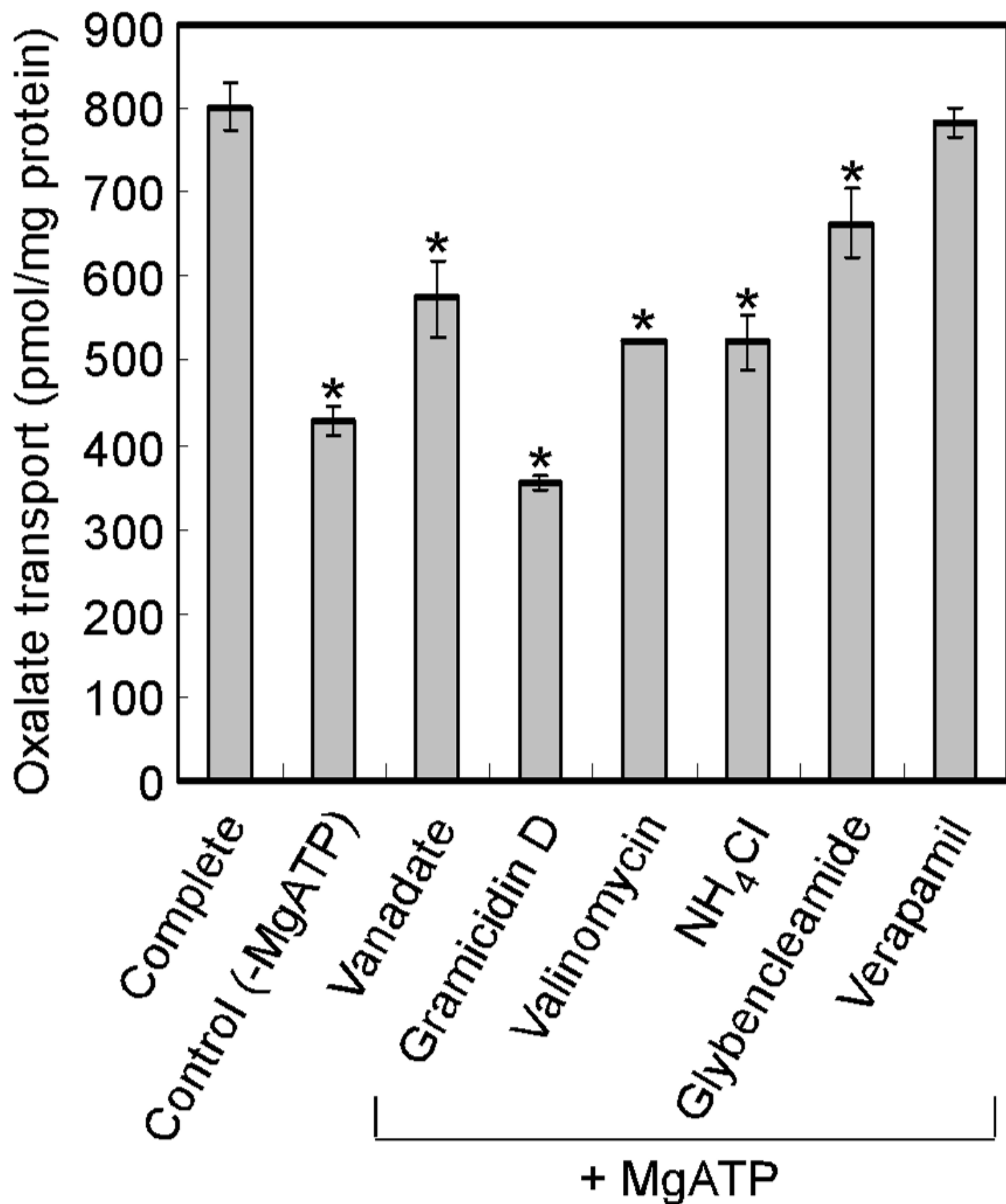


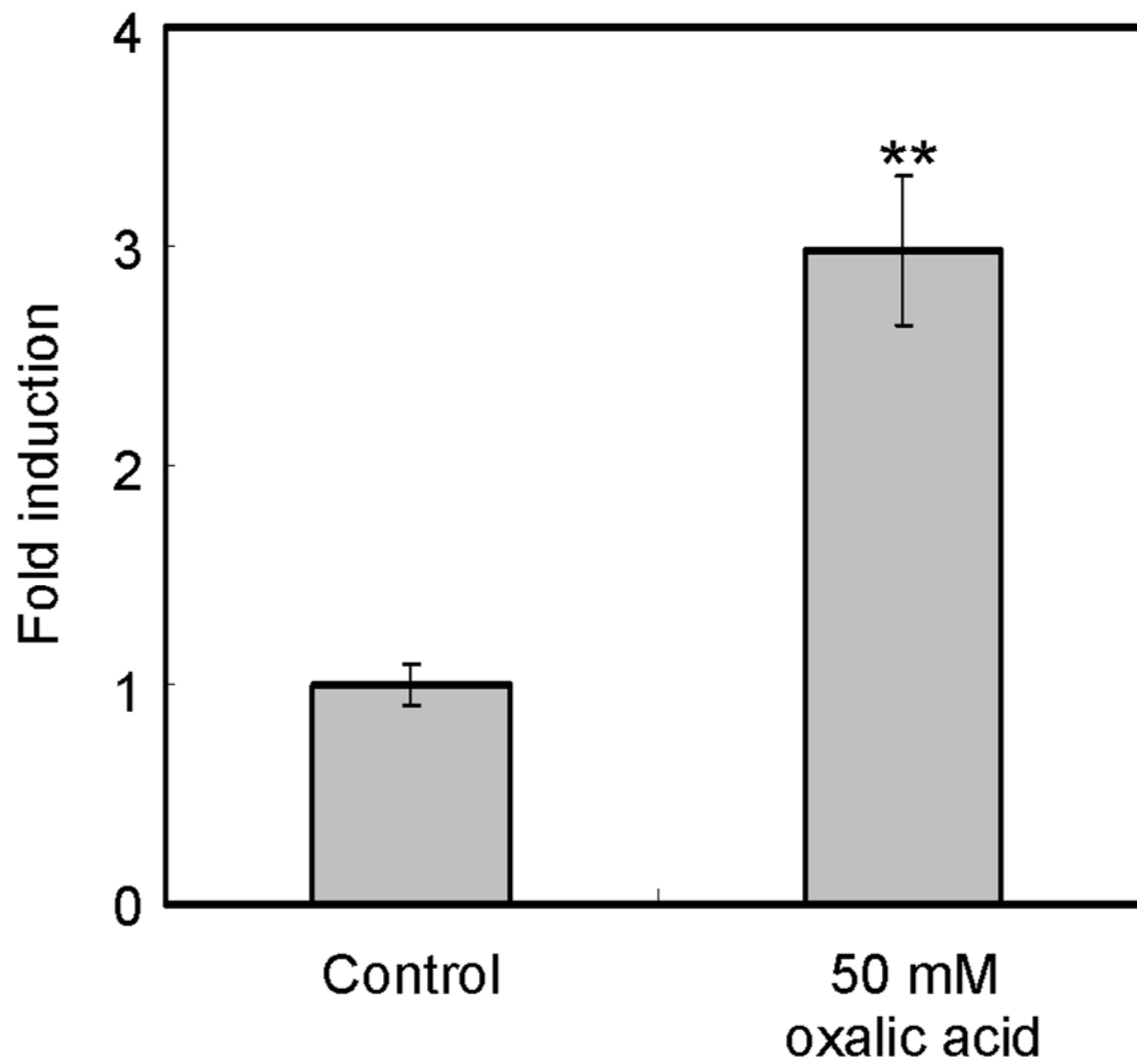
pH1.5

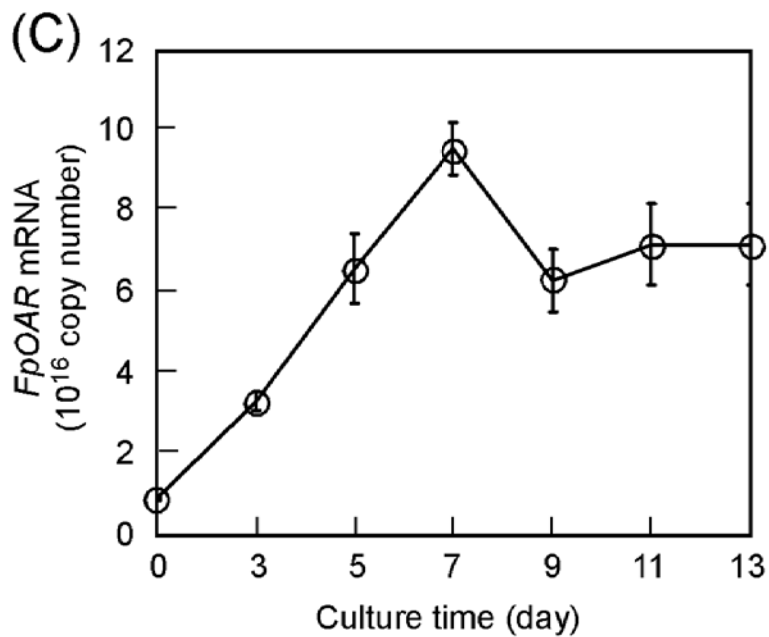
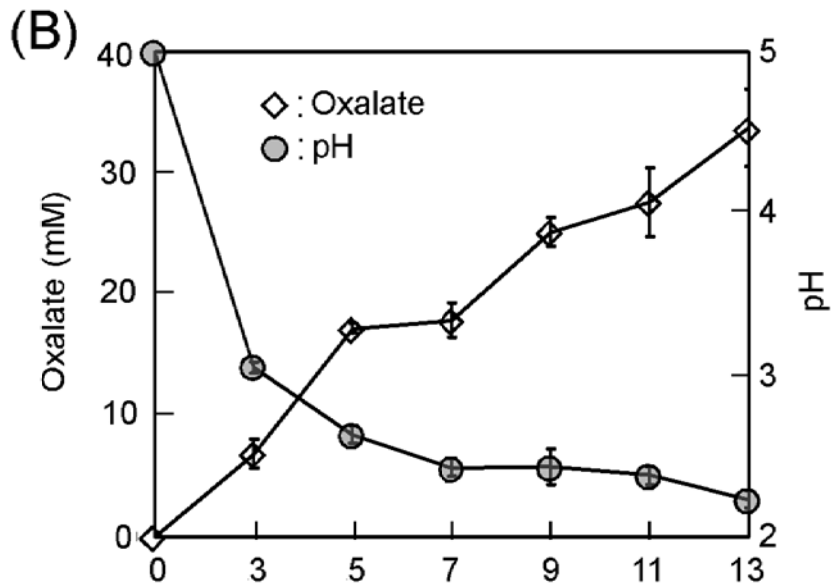
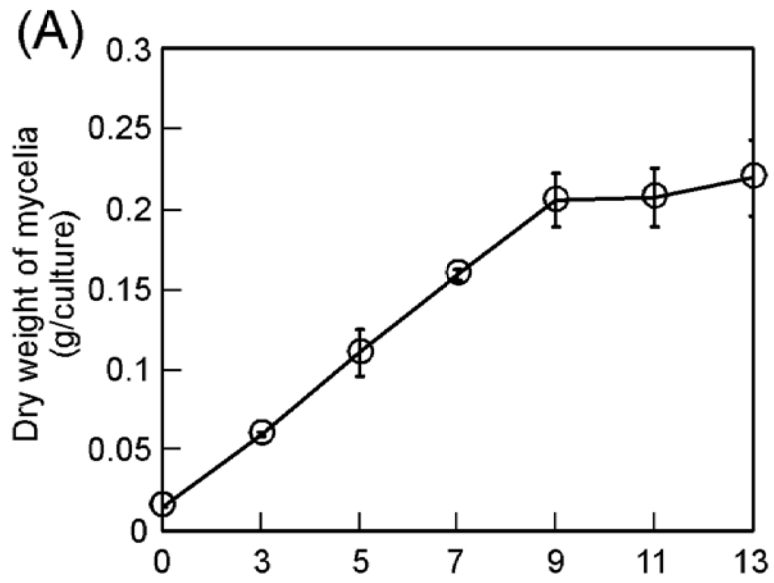












: Primary helix
  : Secondary helix
  : Membrane

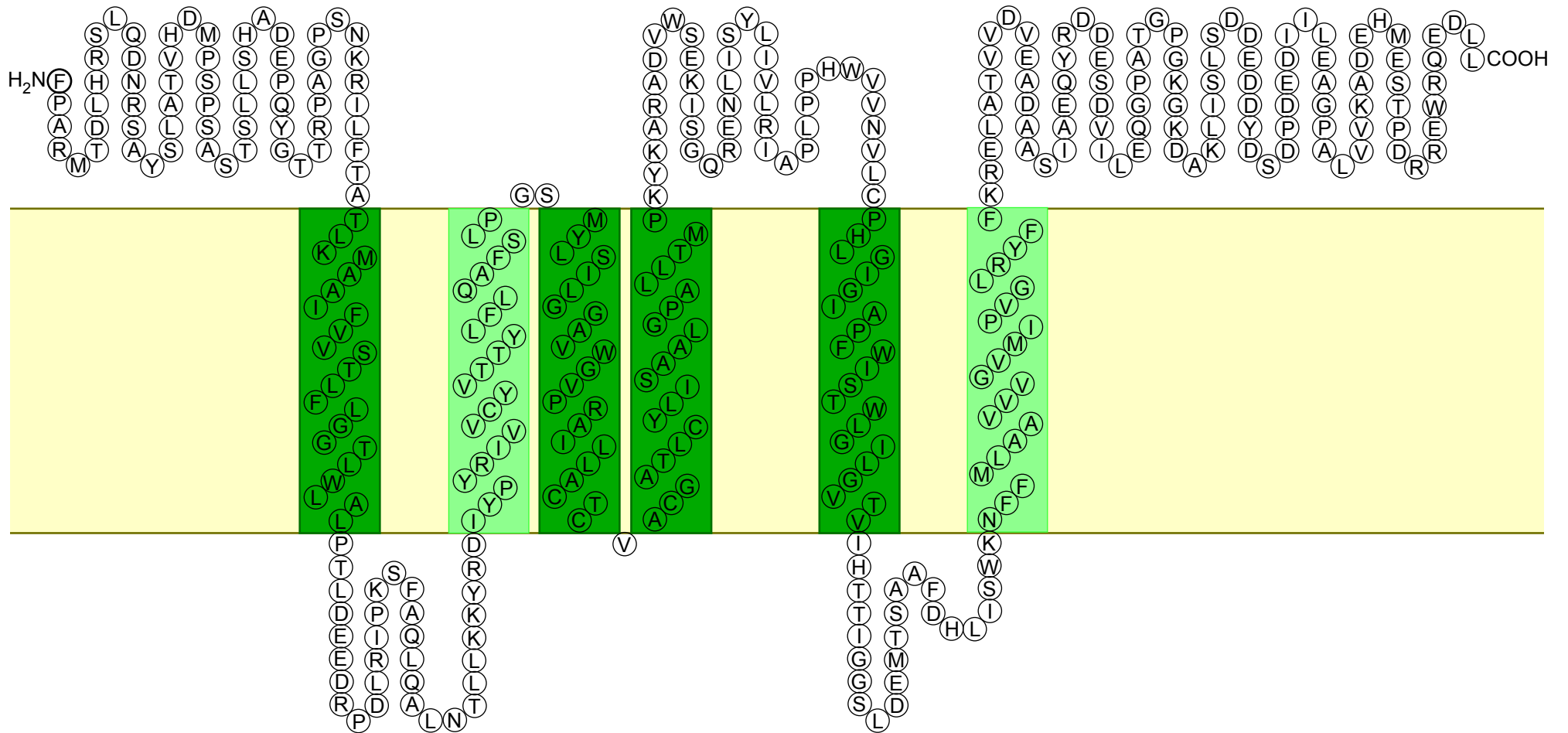


Fig. S1. Predicted transmembrane domains of FpOAR. The prediction was conducted with the SOSUI program (<http://bp.nuap.nagoya-u.ac.jp/sosui/>). The predicted transmembrane domains are shown as primary and secondary helices.